

on the LUMO energy which should be affected by ligand substitution in the same way.

We find that a similar additivity principle is approximately obeyed by the two series of complexes  $[\text{Ni}(\text{dpe})_{2-n}(\text{S}_2\text{CNR}_2)_n]^{(2-n)+}$  and  $[\text{Ni}(\text{dpe})_{2-n}(\text{CN})_2\text{C}_2\text{S}_2]_n]^{(2-2n)+}$  ( $n = 0-2$ ). The reduction potentials for these compounds as a function of  $n$  are given in Figure 11. It is clear from this diagram that the reduction potential varies in an approximately linear manner with  $n$ , where results for the  $n = 0-2$  complexes are available (the dpe series). The results for the  $n = 1$  compounds show that replacement of one dithiolate ligand in the bis(dithiolate) complexes by two molecules of  $\text{PPh}_3$  cause the reduction to shift to considerably more positive potentials than does the corresponding replacement by bis(diphenylphosphino)ethane.

So that the additivity principle for the  $[\text{Ni}(\text{PPh}_3)_{2(2-n)}(\text{R}_2\text{NCS}_2)_n]^{(2-n)+}$  and  $[\text{Ni}(\text{PPh}_3)_{2(2-n)}((\text{CN})_2\text{C}_2\text{S}_2)_n]^{(2-2n)+}$  complexes could be tested, the potential for the one-electron reduction of  $[\text{Ni}^{\text{II}}(\text{PPh}_3)_4]^{2+}$  is required. Extrapolation of the lines through the  $n = 1$  and 2 points to  $n = 0$  suggests that this should occur at a potential of +0.2 V (Figure 11). The reduction of  $\text{Ni}^{2+}$  in the presence of excess  $\text{PPh}_3$  in acetonitrile has been studied by other workers, but the reduction appears to involve the species  $[\text{Ni}^{\text{II}}(\text{PPh}_3)_2(\text{CH}_3\text{CN})_4]^{2+}$  and is a two-electron process which results in the formation of the zerovalent complex  $\text{Ni}(\text{PPh}_3)_4$ . This then reacts with the  $\text{Ni}^{\text{II}}$  complex present to produce  $[\text{Ni}^{\text{I}}(\text{PPh}_3)_4]^+$ , which can be irreversibly oxidized at a potential of about +0.4 V relative to SCE.<sup>31</sup> In an attempt to observe the reversible one-electron reduction of  $[\text{Ni}^{\text{II}}(\text{PPh}_3)_4]^{2+}$ , we carried out similar experiments in  $\text{CH}_2\text{Cl}_2$ , which has a lower coordinating ability than  $\text{CH}_3\text{CN}$ . However, even in the presence of a very large excess of  $\text{PPh}_3$ , the redox behavior was found to be similar to that in  $\text{CH}_3\text{CN}$ . The cathodic peak due to the irreversible oxidation of  $[\text{Ni}^{\text{I}}(\text{PPh}_3)_4]^+$  occurs at +0.23 V, near to the value predicted in Figure 11 for the reversible process.

The greater ease of reduction (i.e., the less negative reduction potential) of the bis(triphenylphosphine) complexes compared with the dpe complexes may be related to the relative strength of the metal-phosphorus interactions. The reduction potential is determined, in part, by the energy of the LUMO which the electron occupies after electron transfer. If the LUMO is high in energy, a greater free energy change

occurs on reduction at a more negative reduction potential.<sup>32</sup> The ESR parameters for the  $\text{Ni}^{\text{I}}$  complexes produced on reduction of the corresponding  $\text{Ni}^{\text{II}}$  complexes suggest that the degree of  $\sigma$ -covalent bonding is greater in the dpe than  $\text{PPh}_3$  compounds. If this is also true, the LUMO occupied by the unpaired electron on reduction is *higher* in energy for the dpe complexes, leading to a *more negative* reduction potential than the corresponding  $\text{PPh}_3$  complexes. While this explanation appears to describe well these results, a great many other factors may also affect the reduction potentials (such as metal phosphorus  $\pi$  interactions and differing solvation energies of oxidized and reduced species). A more complete discussion should take into consideration the change in total electronic energy of the complex as it goes from  $\text{Ni}^{\text{II}}$  to  $\text{Ni}^{\text{I}}$  rather than considering the energy of a single orbital in the parent  $\text{Ni}^{\text{II}}$  complex. However, in the spirit of the frozen-orbital approximation, it is possible to relate total energy changes to changes in single-orbital occupancy.

**Acknowledgment.** We wish to thank the New Zealand University Grants Committee and the New Zealand Energy Research and Development Committee for financial assistance. We also wish to thank Dr. G. A. Wright for the use of electrochemical equipment.

**Registry No.**  $\text{Ni}(\text{dpm})((\text{CN})_2\text{C}_2\text{S}_2)$ , 81097-94-1;  $\text{Ni}(\text{dae})((\text{CN})_2\text{C}_2\text{S}_2)$ , 81097-95-2;  $\text{Ni}(\text{dpe})((\text{CN})_2\text{C}_2\text{S}_2)$ , 81097-96-3;  $\text{Ni}(\text{dpe})(\text{O}_2\text{C}_2\text{S}_2)$ , 81097-97-4;  $\text{Ni}(\text{dpe})(\text{CS}_3)$ , 81097-98-5;  $\text{Ni}(\text{dpe})(\text{CH}_3\text{C}_6\text{H}_3\text{S}_2)$ , 81097-99-6;  $\text{Ni}(\text{dpe})(\text{C}_6\text{H}_4(\text{CH}_2\text{S}_2)_2)$ , 81098-00-2;  $\text{Ni}(\text{dpe})(\text{C}_6\text{H}_4\text{O}_2)$ , 79948-89-3;  $\text{Ni}(\text{dpe})(\text{CH}_3\text{C}_6\text{H}_3\text{O}_2)$ , 81098-01-3;  $\text{Ni}(\text{dpe})(t\text{-BuC}_6\text{H}_3\text{O}_2)$ , 81098-02-4;  $\text{Ni}(\text{dpe})(\text{C}_6\text{Cl}_4\text{O}_2)$ , 38107-43-6;  $\text{Ni}(\text{dpb})((\text{CN})_2\text{C}_2\text{S}_2)$ , 81098-03-5;  $\text{Ni}(\text{PPh}_3)_2((\text{CN})_2\text{C}_2\text{S}_2)$ , 81098-04-6;  $[\text{Ni}(\text{PPh}_3)_2(\text{Et}_2\text{NCS}_2)]^+$ , 55060-26-9;  $[\text{Ni}(\text{PPh}_3)_2(\text{Bu}_2\text{NCS}_2)]^+$ , 55060-27-0;  $[\text{Ni}(\text{PPh}_3)_2(\text{Bzl}_2\text{NCS}_2)]^+$ , 81098-05-7;  $[\text{Ni}(\text{PPh}_3)_2(\text{Cy}_2\text{NCS}_2)]^+$ , 81098-06-8;  $[\text{Ni}((\text{CN})_2\text{C}_2\text{S}_2)_2]^{2-}$ , 14876-79-0;  $\text{Ni}(\text{PPh}_3)_2(\text{Et}_2\text{NCS}_2)$ , 81141-90-4;  $\text{Ni}(\text{PPh}_3)_2(\text{Bu}_2\text{NCS}_2)$ , 81195-35-9;  $\text{Ni}(\text{PPh}_3)_2(\text{Bzl}_2\text{NCS}_2)$ , 81157-73-5;  $\text{Ni}(\text{PPh}_3)_2(\text{Cy}_2\text{NCS}_2)$ , 81098-07-6;  $[\text{Ni}(\text{PPh}_3)_2((\text{CN})_2\text{C}_2\text{S}_2)]^-$ , 81098-08-0;  $[\text{Ni}(\text{dpe})((\text{CN})_2\text{C}_2\text{S}_2)]^-$ , 81098-09-1;  $[\text{Ni}(\text{dpm})((\text{CN})_2\text{C}_2\text{S}_2)]^-$ , 81098-10-4;  $[\text{Ni}(\text{dpb})((\text{CN})_2\text{C}_2\text{S}_2)]^-$ , 81098-11-5;  $[\text{Ni}(\text{dae})((\text{CN})_2\text{C}_2\text{S}_2)]^-$ , 81098-12-6;  $[\text{Ni}(\text{dpe})(\text{CH}_3\text{C}_6\text{H}_3\text{S}_2)]^-$ , 81098-13-7;  $[\text{Ni}(\text{dpe})(\text{O}_2\text{C}_2\text{S}_2)]^-$ , 81098-14-8;  $[\text{Ni}(\text{dpe})(\text{CS}_3)]^-$ , 81098-15-9;  $[\text{Ni}(\text{dpe})(\text{C}_6\text{Cl}_4\text{O}_2)]^-$ , 81098-16-0;  $[\text{Ni}(\text{dpe})(\text{C}_6\text{H}_4\text{O}_2)]^-$ , 81098-17-1;  $[\text{Ni}(\text{dpe})(\text{C}_6\text{H}_3\text{O}_2)]^+$ , 81098-18-2;  $[\text{Ni}(\text{dpe})(\text{CH}_3\text{C}_6\text{H}_3\text{O}_2)]^+$ , 81098-19-3;  $[\text{Ni}(\text{dpe})(t\text{-BuC}_6\text{H}_3\text{O}_2)]^+$ , 81098-20-6;  $[\text{Ni}(\text{dpe})(\text{C}_6\text{Cl}_4\text{O}_2)]^+$ , 81098-21-7;  $\text{Ni}(\text{dpe})\text{Cl}_2$ , 14647-23-5.

(31) Bontempelli, G.; Magno, F.; Corain, B.; Schiavon, G. *J. Electroanal. Chem. Interfacial Electrochem.* 1979, 103, 243.

(32) Bard, A. J.; Faulkner, L. R. "Electrochemical Methods"; Wiley: New York, 1980; Chapter 1.

Contribution from the Department of Chemistry, University of California, Davis, California 95616

## Preparation and Characterization of Some Hydroxy Complexes of Iron(III) Porphyrins

RU-JEN CHENG, LECHOSLAW LATOS-GRAZYNSKI, and ALAN L. BALCH\*

Received December 1, 1981

Oxidation of  $(\text{TMP})\text{Fe}^{\text{II}}$  or  $(\text{T}(2,4,6\text{-MeO})_3\text{PP})\text{Fe}^{\text{II}}$  ( $\text{TMP}$  is the dianion of *meso*-tetramesitylporphyrin;  $\text{T}(2,4,6\text{-MeO})_3\text{PP}$  is the dianion of *meso*-tetrakis(2,4,6-trimethoxyphenyl)porphyrin) yields  $(\text{TMP})\text{FeOH}$  or  $(\text{T}(2,4,6\text{-MeO})_3\text{PP})\text{FeOH}$ . These same hydroxy complexes are obtained by treating the corresponding  $\text{PFe}^{\text{III}}\text{Cl}$  ( $\text{P}$  is a generalized porphyrin dianion) with aqueous sodium hydroxide. Complexes of the type  $\text{PFeOH}$  are distinguished from the more common oxo-bridged dimers  $\text{PFeOFeP}$  on the basis of  $^1\text{H}$  NMR spectra, magnetic susceptibilities, infrared spectroscopy, and electron spin resonance spectroscopy. These hydroxy complexes behave as typical high-spin, five-coordinate iron(III) compounds. Mixtures of  $\text{PFeOH}$  and  $\text{PFeOFeP}$  are formed when  $\text{P}$  is *meso*-tetrakis(3,4,5-trimethoxyphenyl)porphyrin dianion or *meso*-tetrakis(perfluorophenyl)porphyrin dianion.

### Introduction

Iron(III) porphyrin compounds of the type  $\text{PFeX}$  are high-spin ( $S = 5/2$ ), five-coordinate complexes. In the late

1960s it was realized that complexes previously formulated as the hydroxy compounds  $\text{PFeOH}$ , and believed then to be members of the class of  $\text{PFeX}$  compounds, were actually

Table I. Chemical Shifts (ppm) from the  $^1\text{H}$  NMR Spectra of Iron(III) Porphyrins

compd	pyrrole <sup>d</sup>	phenyl substituents <sup>a</sup>		
		ortho	meta	para
(TPP)FeCl	80.8 (250 ± 15) <sup>b</sup>	5.1, 7.7	11.6, 12.7	6.2
(TMP)FeCl <sup>c</sup>	80.3 (330 ± 20)	3.8, 6.5	14.4, 16.0	4.2
(T(2,4,6-MeO) <sub>3</sub> PP)FeCl <sup>c</sup>	78.8 (430 ± 30)	3.21, ~5.2	12.4, 13.7	4.9
(T(3,4,5-MeO) <sub>3</sub> PP)FeCl	80.7 (330 ± 20)	8.5	3.8, 4.3	4.9
(T(F <sub>3</sub> )PP)FeCl	81.6 (330 ± 20)			
(TMP)FeOH <sup>d</sup>	79.2 (535 ± 25)		11.1, 12.0	3.3
(T(2,4,6-MeO) <sub>3</sub> PP)FeOH <sup>d,e</sup>	78.6 (750 ± 30)	3.55, 4.13	10.35, 11.49	4.6
(T(3,4,5-MeO) <sub>3</sub> PP)FeOH <sup>d</sup>	80.2 (550 ± 25)		3.7, 4.0	4.6
(T(F <sub>3</sub> )PP)FeOH <sup>d</sup>	81.2 (550 ± 25)			
[(TPP)Fe] <sub>2</sub> O	13.6	7.9	7.7	7.5
[(T(3,4,5-MeO) <sub>3</sub> PP)Fe] <sub>2</sub> O	13.7		3.2, 4.2	4.2
[(T(F <sub>3</sub> )PP)Fe] <sub>2</sub> O	14.0			

<sup>a</sup> At 25 °C in toluene-*d*<sub>6</sub> with tetramethylsilane as reference unless indicated otherwise. <sup>b</sup> Line width at half-height in Hz. <sup>c</sup> In chloroform-*d*. <sup>d</sup> An additional resonance due to water may be seen at 0 to -2 ppm. Its intensity and chemical shift depend on the amount of water present. <sup>e</sup> In acetone-*d*<sub>6</sub>.

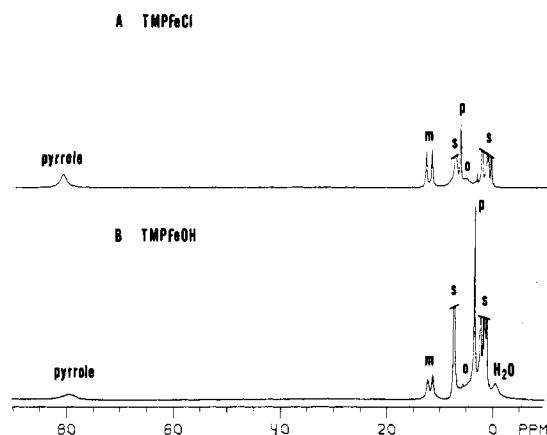
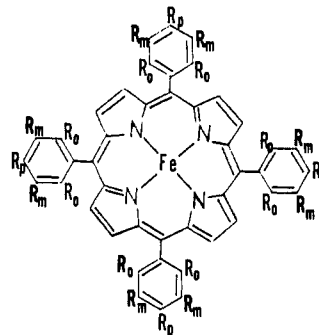


Figure 1.  $^1\text{H}$  NMR spectra of (A) (TMP)FeCl and (B) (TMP)FeOH in toluene-*d*<sub>6</sub> solution at 25 °C. Some of the resonance due to incompletely deuterated solvent (S) have been cut off in intensity.

oxo-bridged complexes PFeOFeP.<sup>1-10</sup> These compounds are also five-coordinate, but strong antiferromagnetic coupling between the two iron(III) ions results in substantially lower magnetic susceptibilities for PFeOFeP than for PFeX. Complexes of the type PFeOFeP have been prepared by two routes: the oxidation of PFe<sup>II</sup> by dioxygen and metathesis of PFeX with hydroxide.

Recent studies in our laboratory involving the detection of reactive intermediates which result from the reaction of iron(II) porphyrins with dioxygen have utilized symmetrically protected (double-picket-fence) porphyrins to prohibit the formation of oxo- and peroxy-bridged porphyrin complexes.<sup>11-15</sup>

For some of these porphyrins, the inability to form PFeOFeP allows stable hydroxy complexes to form.<sup>16</sup> Here we present results of the spectroscopic analysis of the products obtained for both dioxygen oxidation of iron(II) porphyrins and the metathesis of PFeCl with hydroxide for the hindered porphyrins 1-4. Hydroxy complexes are formed by both routes



- 1:  $R_o = R_p = \text{CH}_3$ ,  $R_m = \text{H}$ ; (TMP)Fe<sup>II</sup>
- 2:  $R_o = R_p = \text{OCH}_3$ ,  $R_m = \text{H}$ ; (T(2,4,6-MeO)<sub>3</sub>PP)Fe<sup>II</sup>
- 3:  $R_m = R_p = \text{OCH}_3$ ,  $R_o = \text{H}$ ; (T(3,4,5-MeO)<sub>3</sub>PP)Fe<sup>II</sup>
- 4:  $R_o = R_m = R_p = \text{F}$ ; (T(F<sub>3</sub>)PP)Fe<sup>II</sup>

for 1 and 2, while for 3 and 4 these routes yield mixtures of PFeOH and PFeOFeP, which are related by reaction 1.



The  $^1\text{H}$  NMR spectra of both PFeX<sup>17-21</sup> and PFeOFeP<sup>10,17,22</sup> have been extensively analyzed and serve as excellent means of product identification. Species of the type PFeX are characterized by large downfield shifts of the pyrrole resonance (at ca. 80 ppm at 25 °C) and a meta phenyl doublet (at ~12 ppm at 25 °C). The deviations from Curie law behavior in

- (1) Abbreviations used: P = porphyrin dianion, X = monoanionic ligand, e.g., Cl<sup>-</sup> or OH<sup>-</sup>, TPP = tetraphenylporphyrin dianion.
- (2) Alben, J. O.; Fuchsman, W. H.; Beaudreau, C. A.; Caughey, W. S. *Biochemistry* **1968**, *7*, 624.
- (3) Sadasivan, N.; Eberspaecher, H. I.; Fuchsman, W. H.; Caughey, W. S. *Biochemistry* **1969**, *8*, 534.
- (4) Cohen, I. A. *J. Am. Chem. Soc.* **1969**, *91*, 1980.
- (5) Fleischer, E. B.; Srivastava, T. S. *J. Am. Chem. Soc.* **1969**, *91*, 2403.
- (6) Maricondi, C.; Swift, W.; Straub, D. K. *J. Am. Chem. Soc.* **1969**, *91*, 5205.
- (7) Fleischer, E. B.; Palmer, J. M.; Srivastava, T. S.; Chatterjee, A. *J. Am. Chem. Soc.* **1971**, *93*, 3162.
- (8) Hoffman, A. B.; Collins, D. M.; Day, V. W.; Fleischer, E. B.; Srivastava, T. S.; Hoard, J. L. *J. Am. Chem. Soc.* **1972**, *94*, 3620.
- (9) Murray, K. S. *Coord. Chem. Rev.* **1974**, *12*, 1.
- (10) O'Keefe, D. H.; Barlow, C. H.; Smythe, G. A.; Fuchsman, W. H.; Moss, T. H.; Lilienthal, H. R.; Caughey, W. S. *Bioinorg. Chem.* **1975**, *5*, 125.
- (11) Chin, D.-H.; Del Gaudio, J.; La Mar, G. N.; Balch, A. L. *J. Am. Chem. Soc.* **1977**, *99*, 5486.
- (12) Chin, D.-H.; Balch, A. L.; La Mar, G. N. *J. Am. Chem. Soc.* **1980**, *102*, 1446.

- (13) Chin, D.-H.; La Mar, G. N.; Balch, A. L. *J. Am. Chem. Soc.* **1980**, *102*, 4344.
- (14) Chin, D.-H.; Latos-Grazynski, L.; La Mar, G. N.; Balch, A. L., submitted for publication.
- (15) Latos-Grazynski, L.; Cheng, R.-J.; La Mar, G. N.; Balch, A. L. *J. Am. Chem. Soc.*, in press.
- (16) Other brief reports of the formation of sterically protected forms of PFeOH, including (TMP)FeOH, have appeared: (a) Cense, J. M.; Le Quan, R.-M. *Tetrahedron Lett.* **1979**, 3725. (b) Groves, J. T.; Haushalter, R. C.; Nakamura, M.; Nemo, T. E.; Evans, B. J. *J. Am. Chem. Soc.* **1981**, *103*, 2884. (c) Gunter, M. J.; Mander, L. N.; Murray, K. S. *J. Chem. Soc., Chem. Commun.* **1981**, 799.
- (17) La Mar, G. N.; Eaton, G. R.; Holm, R. H.; Walker, F. A. *J. Am. Chem. Soc.* **1973**, *95*, 63.
- (18) Walker, F. A.; La Mar, G. N. *Ann. N.Y. Acad. Sci.* **1973**, *206*, 328.
- (19) La Mar, G. N.; Walker, F. A. *J. Am. Chem. Soc.* **1973**, *95*, 6950.
- (20) La Mar, G. N.; Walker, F. A. *J. Am. Chem. Soc.* **1975**, *97*, 5103.
- (21) Snyder, R. V.; La Mar, G. N. *J. Am. Chem. Soc.* **1976**, *98*, 4419.
- (22) Wicholas, M.; Mustacich, R.; Jayne, D. *J. Am. Chem. Soc.* **1972**, *94*, 4518.

the temperature dependence of these  $^1\text{H}$  NMR spectra have been analyzed in terms of the zero-field splitting. For  $\text{PFeOFeP}$  the pyrrole resonance occurs in the vicinity of 13.6 ppm at 25 °C, and its temperature dependence gives clear evidence of antiferromagnetism with increasing temperature causing increased isotropic shifts.

## Results

A uniform set of conditions have been employed for preparing and analyzing the (oxo/hydroxy)iron(III) porphyrins. For metathetical reactions with hydroxide, a toluene solution of  $\text{PFeCl}$  was stirred for 2 days with an excess of aqueous sodium hydroxide. After separation of the toluene layer, the iron porphyrin was precipitated from it by the addition of heptane. In some cases further purification was achieved by recrystallization or, in one case, chromatography. With  $(\text{TPP})\text{FeCl}$  this procedure without further purification yields  $(\text{TPP})\text{FeOFe}(\text{TPP})$  and a very small quantity of unreacted  $(\text{TPP})\text{FeCl}$ .<sup>23-25</sup> For the oxidation reaction,  $\text{PFe}^{\text{II}}$ , generated by dithionite reduction of a toluene solution of  $\text{PFeCl}$ ,<sup>26-28</sup> was exposed to dioxygen. The product could be precipitated by addition of heptane, or the solution could be directly subjected to spectroscopic analysis. With  $(\text{TPP})\text{Fe}^{\text{II}}$ , as we have reported earlier, the sole final product that is detected by  $^1\text{H}$  NMR spectroscopy is  $(\text{TPP})\text{FeOFe}(\text{TPP})$ .<sup>11,13</sup>

**(TMP)FeOH.** The product obtained by either the metathesis or the oxidation reaction is  $(\text{TMP})\text{FeOH}$ . The  $^1\text{H}$  NMR spectrum of the product is shown in Figure 1. Its pattern is indicative of the presence of a high-spin, five-coordinate iron(III) complex. The pattern may be compared to that of  $(\text{TMP})\text{FeCl}$ , which is given in Table I along with the  $^1\text{H}$  NMR data for other iron complexes. The assignments shown in Figure 1 are based on relative intensities and comparison with  $(\text{TMP})\text{FeCl}$  and other representatives of the  $\text{PFeX}$  class. The split meta resonance is consistent with the expectations for a five-coordinate complex. All of the line widths are broader than those found for the corresponding chloride complex. In particular, note that the pyrrole resonance of  $(\text{TMP})\text{FeOH}$  is about twice as broad as the corresponding resonance in  $(\text{TMP})\text{FeCl}$ . This is a useful feature in characterizing other hydroxyiron(III) porphyrins. On the other hand, the chemical shift of the pyrrole resonance is not particularly sensitive to the axial anionic ligand as seen for a variety of complexes of the class  $\text{PFe}^{\text{III}}\text{X}$ .<sup>19</sup> The increased line widths of  $(\text{TMP})\text{FeOH}$  result from changes in the zero-field splitting. For these complexes the line width is related to the zero-field splitting parameter  $D$  by eq 2.<sup>19</sup> This yields

$$\delta \propto D^{-2} \quad (2)$$

a value of  $8.9 \text{ cm}^{-1}$  for  $D$  by comparison with the previously determined value of  $11.4 \text{ cm}^{-1}$  for  $(\text{TPP})\text{FeCl}$ .

An additional feature that is a characteristic of the spectra of  $\text{PFeOH}$  is the upfield resonance at  $\sim 0$  ppm, which is ascribed to water. The intensity and position of this peak relative to those of the pyrrole, meta phenyl, and *p*-methyl protons vary from sample to sample. If the sample is shaken with excess

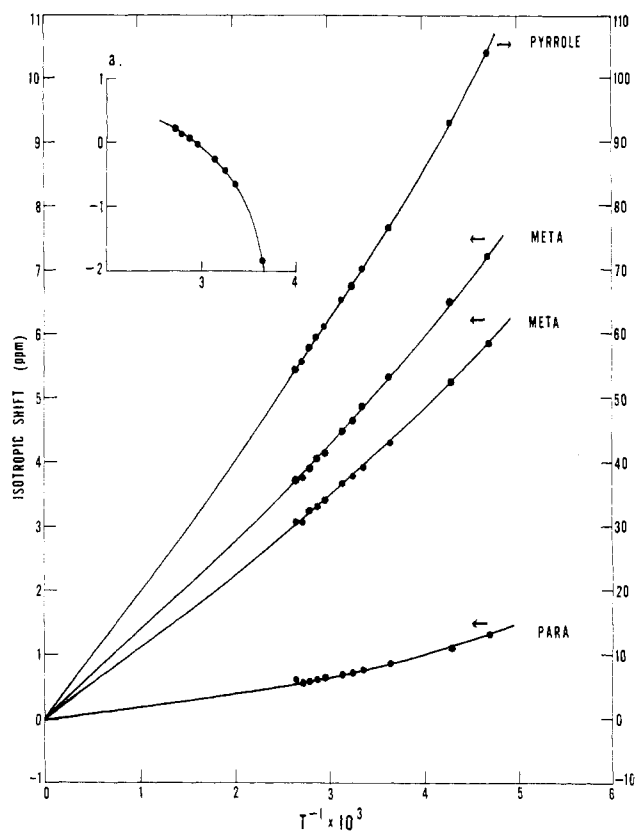


**Figure 2.** Curie plot of the isotropic shifts of  $(\text{TMP})\text{FeOH}$  vs.  $T^{-1}$ . The insert shows the chemical shift of the water resonance as a function of  $T^{-1}$ .

**Table II.**  $g$  Values from the Electron Spin Resonance Spectra of Iron(III) Porphyrins

compd	$g_{\perp}$	$g_{\parallel}$
$(\text{TPP})\text{FeCl}$	5.66	2.03
$(\text{TMP})\text{FeCl}$	5.76	2.05
$(\text{T}(2,4,6\text{-MeO})_3\text{PP})\text{FeCl}$	5.76	2.01
$(\text{T}(3,4,5\text{-MeO})_3\text{PP})\text{FeCl}$	5.66	2.01
$(\text{T}(\text{F}_3)\text{PP})\text{FeCl}$	5.57	2.05
$(\text{TMP})\text{FeOH}$	5.57	2.04
$(\text{T}(2,4,6\text{-MeO})_3\text{PP})\text{FeOH}$	5.74	2.05
$(\text{T}(3,4,5\text{-MeO})_3\text{PP})\text{FeOH} + \text{-O-}$	5.81, 4.29	2.06
$(\text{T}(\text{F}_3)\text{PP})\text{FeOH} + \text{-O-}$	5.66, 4.28	2.00

$\text{D}_2\text{O}$  and then separated from the  $\text{D}_2\text{O}$ , the upfield peak is removed. If toluene saturated with water is added to the sample, the upfield peak shifts further upfield and grows in intensity. The water resonance found in wet toluene usually is present at ca. 1.5 ppm. This is absent from the spectrum in Figure 1. We ascribe the upfield shifts of the water resonance to exchange of protons from the iron-bound hydroxy ligand and water as well as hydrogen bonding, which causes preferential solvation of the water to the hydroxy ligand.

The temperature dependence of the  $^1\text{H}$  NMR spectrum of  $(\text{TMP})\text{FeOH}$  is shown in Figure 2. The behavior is similar to that recorded for  $(\text{TPP})\text{FeCl}$ . The departure from the Curie law is a result of the zero-field splitting and clearly not due to antiferromagnetic coupling. The curvature of the Curie plot can be accounted for by using eq 3, where  $\Delta H/H_0$  is the

$$\Delta H/H_0 = \alpha/T + \beta/T^2 \quad (3)$$

isotropic shift,  $\alpha = -A/h[35g\beta/(12k\gamma_{\text{H}}/2\pi)]$ , and  $\beta = 28g^2\beta^2(3 \cos^2 \theta - 1)D/9k^2r^3$ .<sup>17,18</sup> With use of the computed geometric factors the data can be fit to eq 3 to yield  $A/h = 2.0 \times 10^5 \text{ Hz}$  and  $D = 9.9 \text{ cm}^{-1}$ . The solid lines in Figure 2 are computed with these values. The value of  $D$  is in rea-

(23) We cannot explain a previous report<sup>24</sup> of low (ca. 30%) yields of  $(\text{TPP})\text{FeOFe}(\text{TPP})$  by this route, although we suspect that perhaps the recovery technique involved was inadequate to collect all the product. Higher yields of  $(\text{TPP})\text{FeOFe}(\text{TPP})$  from this method have been reported.<sup>25</sup>

(24) Wollmann, R. G.; Hendrickson, D. N. *Inorg. Chem.* **1977**, *16*, 723.

(25) Baldwin, J. E.; Haraldsson, G. G.; Jones, J. G. *Inorg. Chim. Acta* **1981**, *51*, 29.

(26) Brault, D.; Rougee, M. *Biochemistry* **1974**, *13*, 4591.

(27) Goff, H.; La Mar, G. N.; Reed, C. A. *J. Am. Chem. Soc.* **1977**, *99*, 3641.

(28) The spectroscopic properties of the iron(II) forms of the hindered porphyrins 1-4 are completely consistent with the presence of four-coordinate, intermediate-spin ( $S = 1$ ) iron as found for  $(\text{TPP})\text{Fe}^{\text{II}}$ .<sup>15</sup>

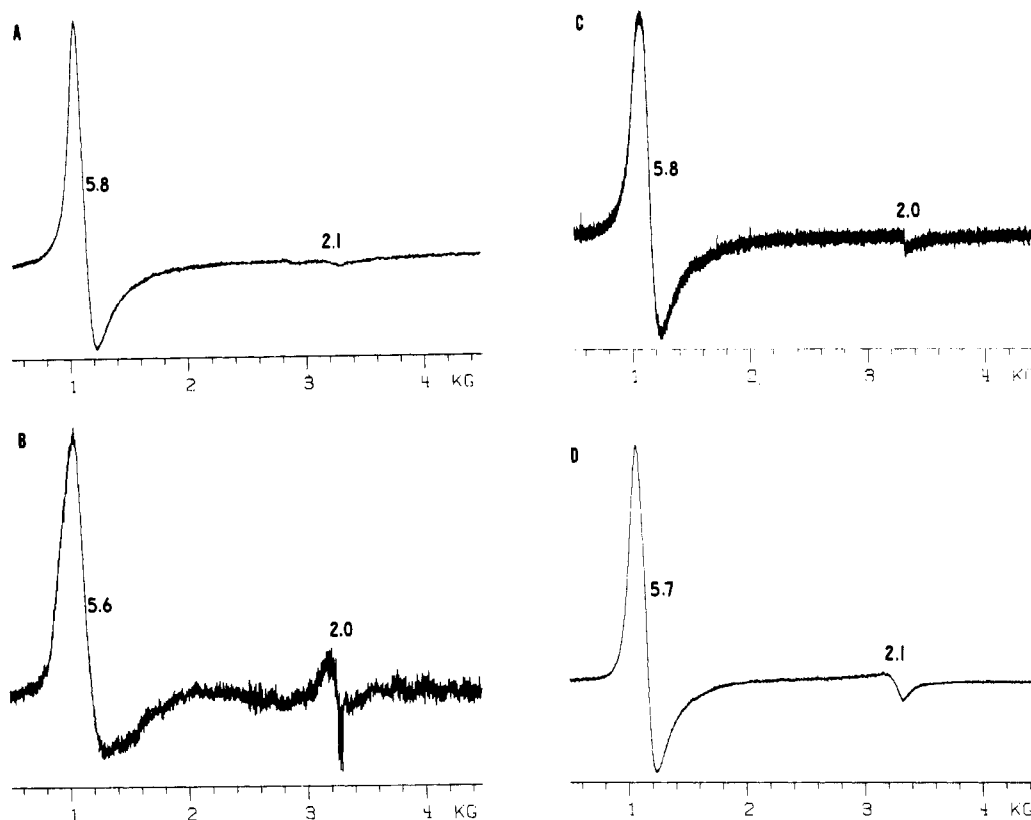


**Figure 3.** Electron spin resonance spectra of frozen toluene solutions at  $-150^{\circ}$  of (A) (TMP)FeCl, (B) (TMP)FeOH, (C) (T(2,4,6-MeO)<sub>3</sub>PP)FeCl, and (D) (T(2,4,6-MeO)<sub>3</sub>PP)FeOH.

**Table III.** Electronic Absorption Spectra of PFe<sup>III</sup>X

(TPP)FeCl	$\lambda$ , nm <sup>a</sup>	419	506	572	656	690
	$\epsilon$ , mM <sup>-1</sup> cm <sup>-1</sup>	133.9	16.4	5.3	3.7	4.4
(TPP)FeOFe(TPP)	$\lambda$ , nm	412		574	610	
	$\epsilon$ , mM <sup>-1</sup> cm <sup>-1</sup>	107		9.2	4.6	
(TMP)FeCl	$\lambda$ , nm	420	508	572	656	694
	$\epsilon$ , mM <sup>-1</sup> cm <sup>-1</sup>	128	14.2	4.7	3.4	3.7
(TMP)FeOH	$\lambda$ , nm	416		580	633	
	$\epsilon$ , mM <sup>-1</sup> cm <sup>-1</sup>	100		7.5	4.4	
(T(2,4,6-MeO) <sub>3</sub> PP)FeCl	$\lambda$ , nm	422	508	578	658	686
	$\epsilon$ , mM <sup>-1</sup> cm <sup>-1</sup>	116	17.7	5.9	4.5	4.1
(T(2,4,6-MeO) <sub>3</sub> PP)FeOH	$\lambda$ , nm	418		578	634	
	$\epsilon$ , mM <sup>-1</sup> cm <sup>-1</sup>	93		7.2	4.0	
(T(3,4,5-MeO) <sub>3</sub> PP)FeCl	$\lambda$ , nm	426	510	574	652	690
	$\epsilon$ , mM <sup>-1</sup> cm <sup>-1</sup>	138	17.4	5.5	3.8	4.3

<sup>a</sup> The wavelength accuracy is  $\pm 2$  nm from 400 to 800 nm.

sonable agreement with that same value calculated on the basis of line widths by using eq 2. Relative to other complexes of the type PFeX, PFeOH has a small  $D$  value.  $D$  values for PFeX increase in the order  $\text{OH}^- < \text{N}_3^- < \text{Cl}^- < \text{Br}^- < \text{I}^-$ .<sup>19</sup>

The magnetic susceptibility of (TMP)FeOH is typical of that of a high-spin Fe(III) species. The magnetic moment measured in toluene solution is  $5.8 \pm 0.1 \mu_B$  over the temperature range  $+25$  to  $-60^{\circ}\text{C}$ .

The ESR spectra of (TMP)FeCl and (TMP)FeOH are shown in Figure 3, and data are collected in Table II. Both spectra show the characteristic features at  $g = 6$  and  $g = 2$  that are expected for PFeX.<sup>29</sup> The hydroxy complex shows additional hyperfine structure at  $g = 2$ . Further analysis of this structure is in progress.

While all of these magnetic measurements are consistent with hydroxy formulation (TMP)FeOH, optical spectroscopy is misleading in identifying this compound. The electronic

spectra of four porphyrins are compared in Figure 4, and numerical data are assembled in Table III. The spectra of (TPP)FeCl and (TMP)FeCl show considerable similarity. While the spectra of (TMP)FeCl and (TMP)FeOH clearly differ, as do the spectra of (TPP)FeCl and (TPP)FeOFe(TPP), there is considerable similarity in the electronic spectra of (TMP)FeOH and (TPP)FeOFe(TPP). These observations, however, are not entirely unexpected. It has been noted earlier that the spectra of (TPP)FeCl and (TPP)FeOCH<sub>3</sub> differ considerably.<sup>30</sup> Moreover the spectra of (TPP)FeOCH<sub>3</sub> and (TPP)FeOFe(TPP) show considerable similarity. An analysis of these spectral variations in terms of configuration interaction admixture of porphyrin triplet and singlet ( $\pi$ ,  $\pi^*$ ) excited states with porphyrin to iron, charge-transfer excited states is available.<sup>30</sup>

(TMP)FeOH has been isolated as a nearly black solid. The analytical data suggest that the solid is a monohydrate. The

(29) Peisach, J.; Blumberg, W. E.; Ogawa, S.; Rachmilewitz, E. A.; Oltzik, R. *J. Biol. Chem.* **1971**, *246*, 3342.

(30) Kobayashi, H.; Higuchi, T.; Kaizu, Y.; Osada, H.; Aoki, M. *Bull. Chem. Soc. Jpn.* **1975**, *48*, 3137.

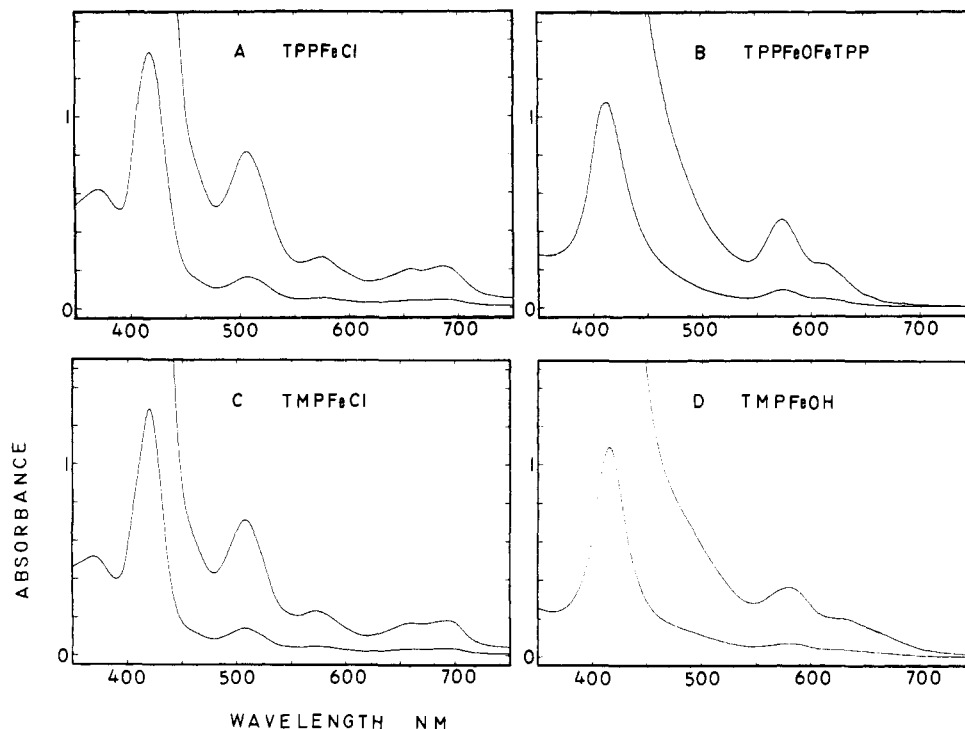


**Figure 4.** Electronic spectra of toluene solutions of (A) (TPP)FeCl, (B) (TPP)FeOFe(TPP), (C) (TMP)FeCl, and (D) (TMP)FeOH. The cell path length was 1.0 mm, and the iron concentration in each case is  $1.0 \times 10^{-4}$  M.

association of water with the hydroxy ligand, which is observed in the NMR spectrum in solution, leads us to suspect that, in the solid state, the water of hydration is intimately involved with the hydroxy group. The infrared spectrum of solid (TMP)FeOH is indicative of a hydroxy complex. A broad O-H absorption is seen at  $3400 \text{ cm}^{-1}$ . There is no evidence for an oxo bridge, which usually displays an antisymmetric Fe-O-Fe stretching vibration at ca.  $850 \text{ cm}^{-1}$ .<sup>4,9,10</sup> The infrared spectrum of (TMP)FeOH shows three sharp bands ( $816 \text{ m}$ ,  $840 \text{ m}$ , and  $854 \text{ w cm}^{-1}$ ) in the  $800\text{--}900 \text{ cm}^{-1}$  region. All three of these features (with the same relative intensities) are found in the spectrum of (TMP)FeCl.

The formation of (TMP)FeOH by metathesis is reversible. When a toluene solution of (TMP)FeOH is shaken with an aqueous solution of hydrogen chloride, (TMP)FeOH is quantitatively converted into (TMP)FeCl. This reaction is also likely to explain the formation of some (TMP)FeCl when (TMP)FeOH is dissolved in ordinary NMR grade chloroform-*d*. For this observation, no precautions were taken to remove hydrogen chloride from the chloroform, and it is probable that the formation of (TMP)FeCl was caused by free hydrogen chloride.

**(T(2,4,6-MeO)<sub>3</sub>PP)FeOH.** The characterization of this compound follows directly from that of (TMP)FeOH. The <sup>1</sup>H NMR spectral parameters are given in Table I. The broad, downfield pyrrole resonance and split meta phenyl protons provide the telling features for identification with the PFeX class. A broad upfield resonance due to water is also observed.

The ESR spectrum of (T(2,4,6-MeO)<sub>3</sub>PP)FeOH shows the characteristic resonances. Data are given in table II and Figure 3. The enhanced intensity of the feature at  $g = 2$  appears to be a general characteristic of the hydroxy complexes.

The infrared spectrum of solid (T(2,4,6-MeO)<sub>3</sub>PP)FeOH shows a broad absorption at  $3350 \text{ cm}^{-1}$  due to the OH stretching vibration. The region from  $800$  to  $900 \text{ cm}^{-1}$  contains a weak band at  $825 \text{ cm}^{-1}$  and a very weak peak at  $962 \text{ cm}^{-1}$ . Both of these features are present in the spectrum of (T(2,4,6-MeO)<sub>3</sub>PP)FeCl. Thus there is no infrared evidence for the presence of an FeOFe unit.

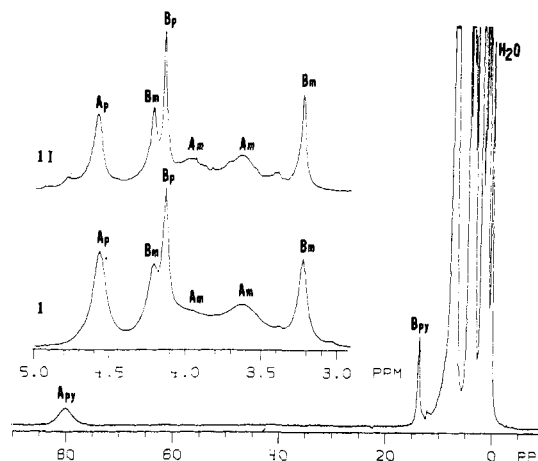


**Figure 5.** <sup>1</sup>H NMR spectrum of the mixture of oxo and hydroxy complexes in toluene-*d*<sub>8</sub> solution at 25 °C formed by the addition of sodium hydroxide to (T(3,4,5-MeO)<sub>3</sub>PP)FeCl. Insert I is an expansion of the 3–5 ppm region of this spectrum. Insert II shows this region for a different sample obtained by the addition of dioxygen to (T(3,4,5-MeO)<sub>3</sub>PP)Fe<sup>II</sup>. Peaks due to (T(3,4,5-MeO)<sub>3</sub>PP)FeOH are labeled A, and those due to (T(3,4,5-MeO)<sub>3</sub>PP)FeOFe(T(3,4,5-MeO)<sub>3</sub>PP) are labeled B. Subscripts identify pyrrole protons (py), *p*-methoxy protons (p), and *m*-methoxy protons (m).

It appears that (T(2,4,6-MeO)<sub>3</sub>PP)FeOH may have been previously prepared by Amundsen and Vaska by oxidation of iron(II).<sup>31,32</sup> They report a magnetic moment of  $5.1 \mu_B$  for a species of uncertain composition that was obtained by oxygenation of what they claimed was diamagnetic (T(2,4,6-MeO)<sub>3</sub>PP)Fe<sup>II</sup>. This latter species has been recently identified as (T(2,4,6-MeO)<sub>3</sub>PP)Fe(pip)<sub>2</sub>.<sup>15</sup>

**(T(3,4,5-MeO)<sub>3</sub>PP)FeOH and (T(3,4,5-MeO)<sub>3</sub>PP)FeOFe(T(3,4,5-MeO)<sub>3</sub>PP).** <sup>1</sup>H NMR analysis indicates that the product of either the oxidation or the metathesis reaction is a mixture of hydroxy and oxo-bridged compounds. Figure

(31) Amundsen, A. R.; Vaska, L. *Inorg. Chim. Acta* 1975, 14, L49.

(32) Amundsen, A. R. Ph.D. Thesis, Clarkson College of Technology, 1976.

5 shows the  $^1\text{H}$  NMR spectrum of this mixture while inserts I and II show expanded portions of the spectra. Insert I was recorded for a sample prepared by metathesis while insert II was recorded for a sample prepared by oxidation of iron(II). All features are present in both figures, and in this case, fortuitously, the relative amounts of the two species appear to be similar. In other samples (vide infra) the relative amounts of the two components vary. From these not only is it clear that two components are present but also assignment of resonances to the two components is simplified. Two resonances in regions expected for pyrrole protons are observed. The broad resonance at 80 ppm is assigned to the pyrrole protons of  $(\text{T}(3,4,5\text{-MeO})_3\text{PP})\text{FeOH}$ . The line width distinguishes the resonance from that of the corresponding chloride (the starting material for metathesis). The resonance at 13.7 ppm is assigned to  $(\text{T}(3,4,5\text{-MeO})_3\text{PP})\text{FeOFe}(\text{T}(3,4,5\text{-MeO})_3\text{PP})$ . The temperature dependence of the chemical shift of this resonance, which changes from 13.7 ppm at 25 °C to 13.1 ppm at -45 °C, is indicative of an antiferromagnetically coupled species. Resonances in the 3–5 ppm region have been assigned on the basis of relative intensities and comparison with the spectrum of  $(\text{T}(3,4,5\text{-MeO})_3\text{PP})\text{FeCl}$ . The temperature dependence of the chemical shift of some peaks also helps to establish their assignment. For example the peak assigned to the *p*-methoxy group in  $(\text{T}(3,4,5\text{-MeO})_3\text{PP})\text{FeOH}$  shifts from 4.9 ppm at -45 °C toward its diamagnetic position so that it is at 4.5 ppm at 25 °C. Notice that an upfield peak characteristic of water in the presence of an iron hydroxy complex is observed.

The ESR spectrum of this mixture has also been recorded. The spectrum shows the features expected for the presence of high-spin  $\text{PFeX}$ . The data are given in Table II. In addition, resonances at  $g \approx 4$  are seen; these may be due to the oxo-bridged species.<sup>33</sup>

The infrared spectrum of the mixture shows evidence of both hydroxy and bridging oxo ligands. A broad absorption at 3400  $\text{cm}^{-1}$  due to the OH stretch is present as is a strong absorption at 865  $\text{cm}^{-1}$ . The infrared spectrum of  $(\text{T}(3,4,5\text{-MeO})_3\text{PP})\text{FeCl}$  lacks the 3400- $\text{cm}^{-1}$  band and contains a strong band at 807  $\text{cm}^{-1}$  and a weak doublet at 856 and 863  $\text{cm}^{-1}$ . In comparison the oxo/hydroxy mixture has a strong band at 812  $\text{cm}^{-1}$ , but the band at 865  $\text{cm}^{-1}$  is the strongest absorption in the 750–950  $\text{cm}^{-1}$  region. Otherwise the patterns of absorptions and their relative intensities are similar for both the oxo/hydroxy mixture and  $(\text{T}(3,4,6\text{-MeO})_3\text{PP})\text{FeCl}$  throughout the 700–1600  $\text{cm}^{-1}$  region. Consequently, for the oxo/hydroxy mixture, the intense 865- $\text{cm}^{-1}$  absorption is assigned to the Fe–O–Fe stretch.

The fractional content of the oxo-bridged component in the mixture can be increased through removing water by azeotropic distillation. However, attempts to reverse this process have not been successful. A sample containing >90% oxo-bridged complex in toluene was shaken for 2 days with excess water. No increase in the amount of hydroxy complex was noted.

**$(\text{T}(\text{F}_5)\text{PP})\text{FeOH}$  and  $(\text{T}(\text{F}_5)\text{PP})\text{FeOFe}(\text{T}(\text{F}_5)\text{PP})$ .** A mixture of hydroxy and oxo-bridged complexes is also produced by either the oxidation or the metathesis reactions involving tetrakis(pentafluorophenyl)porphyrin. The  $^1\text{H}$  NMR spectrum of the product exhibits two pyrrole resonances. The pyrrole resonance of  $(\text{T}(\text{F}_5)\text{PP})\text{FeOH}$  is clearly distinguished from its chloro precursor by its greater line width, while the pyrrole resonance of the oxo-bridged product shows typical antiferromagnetic behavior.

The ESR spectrum of the mixture is also consistent with the presence of a high-spin five-coordinate iron(III) complex.

Because of the small quantity of material available no effort was made to separate the two species.

## Discussion

The existence of hydroxy complexes of iron(III) porphyrins involving the hindered porphyrins 1–4 has been established through a variety of spectroscopic investigations. From our experience  $^1\text{H}$  NMR spectroscopy is the most sensitive and efficient means of detecting the presence of  $\text{PFeOH}$ , particularly in complex reaction mixtures. The stability of  $(\text{TMP})\text{FeOH}$  and  $(\text{T}(2,4,6\text{-MeO})_3\text{PP})\text{FeOH}$  is readily attributed to steric effects, which prohibit the formation of the corresponding oxo-bridged species. In the case of  $(\text{T}(3,4,5\text{-MeO})_3\text{PP})\text{FeX}$  and  $(\text{T}(\text{F}_5)\text{PP})\text{FeX}$  these steric constraints are relaxed to the extent that both hydroxy and oxo-bridged compounds can coexist. The relaxation of the steric constraints is not unexpected. The van der Waals radius of a fluorine atom is 1.35 Å while that of a methyl group is 2.0 Å.<sup>34</sup> Consequently the closer approach of two porphyrin planes is more likely with  $(\text{T}(\text{F}_5)\text{PP})\text{FeX}$  than with  $(\text{TMP})\text{FeX}$ . Moving the methoxy substituents from the 2- and 6- to the 3- and 5-positions on the phenyl ring results in less crowding in the key region immediately adjacent to the Fe–O–Fe link. Doming of the porphyrin in oxo-bridged species results in less steric hindrance as substituents are placed further from the center of the porphyrin. Consequently  $(\text{T}(3,4,5\text{-MeO})_3\text{PP})\text{FeX}$  can form a mixture of oxo-bridged and hydroxy while  $(\text{T}(2,4,6\text{-MeO})_3\text{PP})\text{FeOH}$  exists solely in the hydroxy form.

The hydroxy and oxo-bridged complexes are related by the reaction shown in eq 2. Equilibrium between the two forms appears to be only slowly established. While we have successfully transformed  $(\text{T}(3,4,5\text{-MeO})_3\text{PP})\text{FeOH}$  into  $(\text{T}(3,4,5\text{-MeO})_3\text{PP})\text{FeOFe}(\text{T}(3,4,5\text{-MeO})_3\text{PP})$  by dehydration, the reverse reaction has not been observed. Of course it could be that the oxo-bridged form is the more thermodynamically stable form. The reversible transformation of oxo-bridged and hydroxy complexes has been demonstrated for some molybdenum porphyrin complexes.<sup>35</sup>

## Experimental Section

**Materials.**  $(\text{TMP})\text{H}_2$ ,<sup>36</sup>  $(\text{T}(2,4,6\text{-MeO})_3\text{PP})\text{H}_2$ ,<sup>31,32,37</sup> and  $(\text{T}(\text{F}_5)\text{PP})\text{H}_2$ <sup>38</sup> were prepared by previously reported procedures.  $(\text{T}(3,4,5\text{-MeO})_3\text{PP})\text{H}_2$  was prepared by standard methods starting with 3,4,5-trimethoxybenzaldehyde.<sup>39</sup> Insertion of iron into these porphyrins followed established routes.<sup>40</sup>

**Metathesis Reactions.** A 1 mM toluene solution of  $\text{PFeCl}$  was vigorously stirred with an aqueous sodium hydroxide solution for 1 day. The toluene solution was separated from the mixture by means of pipet, and the solution was evaporated to dryness by using a rotary evaporator. The resulting solid was then redissolved in toluene and filtered, and the iron porphyrin was reprecipitated by the addition of heptane. The solid was collected by filtration and vacuum dried. Anal. Calcd for  $(\text{TMP})\text{FeOH}\cdot\text{H}_2\text{O}$ ,  $\text{C}_{36}\text{H}_{55}\text{N}_4\text{O}_2\text{Fe}$ : C, 77.14; H, 6.36; N, 6.43. Found: C, 76.82; H, 6.56; N, 5.98. Calcd for  $(\text{T}(2,4,6\text{-MeO})_3\text{PP})\text{FeOH}\cdot\text{H}_2\text{O}$ ,  $\text{C}_{56}\text{H}_{55}\text{N}_4\text{O}_{14}\text{Fe}$ : C, 63.22; H, 5.21; N, 5.27. Found: C, 63.99; H, 5.50; N, 4.95.

**Oxygenation Reactions.** Unligated iron(II) porphyrins were prepared by reduction of the appropriate iron(III) complex in toluene

(33) While ESR spectra have been reported for some oxo-bridged iron(III) complexes, these spectra have not been analyzed in detail.<sup>9</sup>

- (34) Pauling, L. "The Nature of the Chemical Bond"; Cornell University Press: Ithaca, NY, 1950; p 260.  
 (35) Ledon, H. J.; Bonnet, M. C.; Brigandat, Y.; Varescon, F. *Inorg. Chem.* **1980**, *19*, 3488.  
 (36) Badger, G. M.; Jones, R. A.; Laslett, R. L. *Aust. J. Chem.* **1964**, *17*, 1028.  
 (37) Vaska, L.; Amundsen, A. R.; Brady, R.; Flynn, B. R.; Nakai, H. *Finn. Chem. Lett.* **1974**, 66.  
 (38) Longo, F. R.; Finarelli, M. G.; Kim, J. B. *J. Heterocycl. Chem.* **1969**, *6*, 927.  
 (39) Adler, A. D.; Longo, F. R.; Finarelli, J. D.; Goldmacher, J.; Assour, J.; Korsakoff, L. *J. Org. Chem.* **1967**, *32*, 476.  
 (40) Adler, A. D.; Longo, F. R.; Kampus, F.; Kim, J. *J. Inorg. Nucl. Chem.* **1970**, *32*, 2443.

or dichloromethane solution with an aqueous sodium dithionite solution in a Keweenaw controlled-atmosphere box under purified nitrogen. Typically 1 mg of iron(III) porphyrin and 5 mg of sodium dithionite were dissolved in a mixture of 0.5 mL of toluene and several drops of water. The solutions were shaken to mix the two layers. After reduction was complete, as noted by a color change from green-brown to red, the two layers were allowed to separate. The aqueous layer was removed by a pipet. The toluene solution was then washed with a fresh sample of deoxygenated water to remove any remaining inorganic salts. The solvent was evaporated from the sample under vacuum, and the sample was dried for 12 h under continuous vacuum. The iron porphyrin was then dissolved in deoxygenated, deuterated toluene and transferred into an NMR tube in the controlled-atmosphere box. The NMR tube was sealed with a septum cap, and dry dioxygen was admitted to the sample. This solution could be used directly for spectroscopic examination. The iron porphyrin could be precipitated by the addition of heptane and collected by filtration.

**Instrumentation.**  $^1\text{H}$  NMR spectra at 200 and 360 MHz were recorded on Nicolet NT-200 and NT-360 FT NMR spectrometers. Between 300 and 2000 transients were accumulated with use of a 90° pulse. Electronic spectra were measured with a Hewlett-Packard 8450A spectrophotometer. Infrared spectra were obtained from Nujol

mulls of the solid complexes. A Perkin-Elmer 180 spectrometer was used to record the spectra. ESR spectra were recorded at the X band with a Bruker spectrometer. Samples were dissolved in toluene, and spectra were obtained from samples cooled to  $-150^\circ\text{C}$ . Magnetic susceptibilities of toluene solutions were measured with use of the Evans technique.<sup>41</sup>

**Acknowledgment.** We thank the National Institutes of Health (Grant No. GM26226) for support and Professor G. N. La Mar for discussions and a sample of  $(\text{T}(\text{F}_5)\text{PP})\text{H}_2$ . L.L.-G. was on leave from the Institute of Chemistry, University of Wrocław, Wrocław, Poland.

**Registry No.**  $(\text{TMP})\text{FeOH}$ , 81245-23-0;  $(\text{T}(2,4,6\text{-MeO})_3\text{PP})\text{-FeOH}$ , 81245-22-9;  $(\text{TPP})\text{FeCl}$ , 16456-81-8;  $(\text{TMP})\text{FeCl}$ , 77439-21-5;  $(\text{T}(2,4,6\text{-MeO})_3\text{PP})\text{FeCl}$ , 53470-05-6;  $(\text{T}(3,4,5\text{-MeO})_3\text{PP})\text{FeCl}$ , 81245-21-8;  $(\text{T}(\text{F}_5)\text{PP})\text{FeCl}$ , 36965-71-6;  $(\text{T}(3,4,5\text{-MeO})_3\text{PP})\text{FeOH}$ , 81278-78-6;  $(\text{T}(\text{F}_5)\text{PP})\text{FeOH}$ , 81278-77-5;  $[(\text{TPP})\text{Fe}]_2\text{O}$ , 12582-61-5;  $[(\text{T}(3,4,5\text{-MeO})_3\text{PP})\text{Fe}]_2\text{O}$ , 81245-19-4;  $[(\text{T}(\text{F}_5)\text{PP})\text{Fe}]_2\text{O}$ , 81245-20-7.

(41) Evans, D. F. *J. Chem. Soc.* 1959, 2003.

Contribution from the Central Leather Research Institute, Adyar, Madras-600 020, India, and the Department of Physical Chemistry, University of Madras, A.C. College Campus, Madras-600 025, India

## Ternary Coordination Complexes of Copper(II) Containing Histamine and Some Amino Acids

MADHAVAN SIVASANKARAN NAIR,\* KORA VENKATACHALAPATHI, MUCHI SANTAPPA, and PULIAMPATTI K. MURUGAN

Received June 16, 1981

Equilibrium constants have been measured by pH titrimetry at  $37^\circ\text{C}$  and  $I = 0.15\text{ mol dm}^{-3}$  ( $\text{NaClO}_4$ ) for some ternary systems,  $\text{Cu}^{\text{II}}\text{AB}$  [ $A = \text{histamine}$ ;  $B = \text{DL-2-aminobutyric acid (2-aba)}$ ,  $\text{DL-3-aminobutyric acid (3-aba)}$ ,  $4\text{-aminobutyric acid (4-aba)}$ ,  $\text{DL-4-amino-3-hydroxybutyric acid (ahba)}$ ,  $\text{DL-2,3-diaminopropionic acid (dapa)}$ ,  $\text{DL-2,4-diaminobutyric acid (daba)}$ , and  $\text{DL-ornithine (Orn)}$ ], in aqueous perchlorate media. Very high stabilities were observed for all types of the ternary complex species  $\text{CuAB}$ ,  $\text{Cu}((\text{AB})\text{H})$ , or  $\text{Cu}((\text{AB})\text{H}_2)$  detected. Copper(II) ternary complexes having six- and five-membered chelate rings are found to be more stable than those having six- and six- or six- and seven-membered chelate rings. It appears from the results that in the presence of histamine ( $A$ )  $dapa$ ,  $daba$ , and  $Orn$  ( $B$ ) bind copper(II) in a tridentate manner, while the other potentially tridentate ligand,  $ahba$  ( $B$ ), coordinates in a bidentate manner. The trends in the  $\text{pK}_{\text{Cu}((\text{AB})\text{H})}^{\text{H}}$  values suggest that the extra proton in the  $\text{Cu}((\text{AB})\text{H})$  complexes is attached to the ligand  $B$ . However, in the systems where  $\text{Cu}((\text{AB})\text{H}_2)$  complexes were detected, the possibility for the attachment of one proton to the histamine ( $A$ ) and the other to the ligand  $B$  was predicted.

### Introduction

Considerable attention has been paid in recent years to the studies of complex-forming properties of histamine, which is of importance from the biological point of view.<sup>1,2</sup> Several workers<sup>3-6</sup> investigated the equilibrium chemistry of copper(II) ternary complexes containing histamine as a ligand. Gergely and Sovago<sup>5</sup> described studies relating to the copper(II)-histamine-amino acid ternary complexes, where the increased stability was explained by a large entropy effect. We have been investigating<sup>7a-c</sup> the stability and structure of ternary complex species of the type  $\text{Cu}((\text{AB})\text{H}_2)$ ,  $\text{Cu}((\text{AB})\text{H})$ ,  $\text{CuAB}$ ,  $\text{Cu}((\text{AB})\text{H}_{-1})$ , or  $\text{CuAB}_2$  in some copper(II)-histamine ( $A$ )-secondary ligand ( $B$ ) systems toward a better understanding of the nature of metal ion complexation in biological processes. In the present paper, we report the equilibrium data for some new copper(II)-histamine ( $A$ )-amino acid ( $B$ ) ternary systems obtained by pH titrimetry at  $37^\circ\text{C}$  and  $I = 0.15\text{ mol dm}^{-3}$  ( $\text{NaClO}_4$ ). The amino acids ( $B$ ) chosen are DL-2-

aminobutyric acid (2-aba), DL-3-aminobutyric acid (3-aba), 4-aminobutyric acid (4-aba), DL-4-amino-3-hydroxybutyric acid (ahba), DL-2,3-diaminopropionic acid (dapa), DL-2,4-diaminobutyric acid (daba), and DL-ornithine (Orn). The amino acids 2-aba, 3-aba, and 4-aba are capable respectively of forming five-, six-, and seven-membered chelate rings with copper(II). The  $ahba$  ligand is potentially tridentate having amino-, hydroxy-, and carboxylate-donor groups. The compounds  $dapa$ ,  $daba$ , and  $Orn$  are diaminocarboxylic acids of general formula  $\text{NH}_2(\text{CH}_2)_n\text{CH}(\text{NH}_2)\text{COOH}$ , where  $n = 1$  ( $dapa$ ), 2 ( $daba$ ), and 3 ( $Orn$ ).

### Experimental Section

All the ligands used were obtained from Fluka. The compounds  $dapa$  and  $Orn$  were used in the monoprotonated form, while  $daba$  was

\* To whom correspondence should be addressed at the Department of Chemistry, Post-Graduate Extension Centre, Madurai Kamaraj University, St. John's College Campus, Palayamkottai-627 002, Tamil Nadu, India.

- (1) R. W. Schayer, "Histamine and Its Role in Biological Systems; Biogenic Amines and Physiological Membranes in Drug Therapy", J. H. Bell and L. G. Abood, Eds., Marcel Dekker, New York, 1971.
- (2) *Met. Ions Biol. Syst.*, 1-9 (1973-1979).
- (3) *Spec. Publ.—Chem. Soc.*, No. 17 (1964); No. 25 (1971).
- (4) D. D. Perrin, I. G. Sayce, and V. S. Sharma, *J. Chem. Soc. A*, 1755 (1967).
- (5) A. Gergely and I. Sovago, *J. Inorg. Nucl. Chem.*, 35, 4355 (1973).
- (6) M. S. Mohan, D. Bancroft, and E. H. Abbott, *Inorg. Chem.*, 18, 1527 (1979).